Queen's University
Belfast

# Multi-method geophysical mapping of quick clay

**Published in:**
Near Surface Geophysics

**Document Version:**
Peer reviewed version

**Queen's University Belfast - Research Portal:**
Link to publication record in Queen's University Belfast Research Portal

# Multi-method geophysical mapping of quick clay

Shane Donohue[1*], Michael Long[2], Peter O'Connor[3], Tonje Eide Helle[5],
Andreas Aspmo Pfaffhuber[4] and Magnus Rømoen[4]

[1] *Dept. of Architecture and Civil Engineering, University of Bath*
[2] *School of Civil, Structural and Environmental Engineering, University College Dublin (UCD)*
[3] *Apex Geoservices*
[4] *Norwegian Geotechnical Institute (NGI)*
[5] *Norwegian Public Roads Administration – Statens Vegvesen*

### ABSTRACT

Marine clay deposits in coastal, post-submarine areas of Scandinavia and North America may be subjected to quick clay landslides and hence significant efforts are being taken to map their occurrence and extent. The purpose of this paper is to assess the use of a number of geophysical techniques for identifying quick clay. The investigated area, Smørgrav, located in southern Norway has a history of quick clay sliding, the most recent event occurring in 1984. Geophysical techniques that are used include electromagnetic conductivity mapping, electrical resistivity tomography, seismic refraction and multichannel analysis of surface waves. These results are compared to geotechnical data from bore samples, rotary pressure soundings and cone penetration testing. A number of these approaches have proved promising for identifying quick clay, in particular electrical resistivity tomography and electromagnetics, which delineated a zone of quick clay that had previously been confirmed by rotary pressure soundings and sampling. Seismic refraction was useful for determining the sediment distribution as well as for indicating the presence of shallow bedrock whereas the multichannel analysis of surface-waves approach suggested differences between the intact stiffness of quick and unleached clay. It is observed that quick clay investigations using discrete rotary pressure soundings can be significantly enhanced by using, in particular, electrical resistivity tomography profiles to link together the information between test locations, perhaps significantly reducing the need for large numbers of soundings.

## INTRODUCTION

Quick clay may be described as highly sensitive marine clay that changes from a relatively stable condition to a liquid mass when disturbed. In Norway, some of the most densely inhabited areas, such as the areas around Oslo and Trondheim are partly located in quick clay and hence large efforts are being taken to map their occurrence and extent. Some examples of major quick clay landslides in Scandinavia that have caused significant damage include the 1957 Göta slide (Rankka *et al*. 2004; Göransson *et al*. 2009), the 1978 Rissa slide (Gregersen 1981) and more recently, the 2009 Namsos slide.

### Quick clay – formation and properties

Quick clays, although marine in origin currently lie above sea level, as a result of isostatic uplift following deglaciation. The original marine depositional environment resulted in a clay with a highly porous, open structure generally containing a high void ratio. The original pore water chemistry of these clays may have been altered as a result of the change from a marine to a freshwater environment. As a result, they may have become highly sensitive or 'quick' if sufficient leaching of salt from the soil pore water occurred. Although leaching does not usually affect the flocculated structure, it can, however, strongly affect the interparticle forces, reducing the capacity of the particles to reflocculate following remoulding (Brenner *et al*. 1981). Remoulding of these materials will therefore result in a low viscosity liquid containing small and separated particles. Leaching may be caused by rainwater infiltration, diffusion and water seeping upwards through the deposit due to artesian pressures. The presence of permeable materials such as silts, sands and gravels will also increase the possibility of leaching. The pore water ion composition may also be an important factor in the formation of quick clay as well as other factors such as pH level and the presence of dispersive agents (Rankka *et al*. 2004).

There are a number of significant differences between the geotechnical properties of quick and non-quick clays. Bjerrum

* S.Donohue@bath.ac.uk

(1954) studied the effect of leaching on a number of these properties. In Norway, clay may be considered quick when it has a remoulded shear strength of less than 0.5 kPa. Quick clay also usually exhibits a sensitivity (intact strength/remoulded strength) of greater than 30. As the clay particles may not be able to form large aggregates following remoulding, the water holding capacity of the clay (reflected in the liquid limit, $w_L$), will therefore be reduced. Torrance (1974) suggested that the salt content, which has a major influence on resistivity, has to be reduced below 2 g/l before quick clay can be formed, although more recently, Andersson-Sköld *et al.* (2005) measured a salinity of 5.6 g/l in a Swedish quick clay. Non-quick marine clay may also contain a very low salt content due to continued leaching or weathering. As a result, Andersson-Skold *et al.* (2005) suggested that quick clay should not be distinguished on salinity alone. Quick clays are also characterized as being rich in non-swelling clay minerals.

**Quick clay mapping**

In Norway, the methodology generally used for identifying the presence of quick clay involves using rotary pressure soundings or total soundings sampled at uniform intervals along a slope under investigation. These approaches use purpose built drill tips attached to sounding rods that are simply pushed at a constant rate into the ground while simultaneously rotating, also at a constant rate. If the slope of the penetration resistance curve from either of these soundings is constant or decreasing (indicating a very low remoulded strength) the material is designated as very sensitive or quick clay, according to Rygg (1988). The actual sensitivity is then checked using field vane tests or on samples in the laboratory. The use of rotary pressure or total soundings and vane testing in this manner is considered very reliable for assessing quick clay, however they may be expensive and time consuming and only provide discrete information.

Recently there has been some work published on the use of geoelectrical measurements for mapping quick clay. These field studies have compared measured resistivity values with salt content (Söderblom 1969; Solberg *et al.* 2008), as well as remoulded strength and sensitivity (Rankka *et al.* 2004; Dahlin *et al.* 2005; Lundström *et al.* 2009). Unleached marine clay, which maintains a large concentration of ions in its pore water, has been shown to have very low values of resistivity, generally less than 10 Ωm. On the other hand, for quick clay, where significant leaching of salt has occurred, the resistivity values would be expected to be higher than that of the unleached clay. A recent criterion developed by Solberg *et al.* (2008), suggests that marine clay may be quick if it has a resistivity in the 10–80 Ωm range and that unleached marine clay generally exhibits resistivity values less than 10 Ωm. Resistivity values in the 10–80 Ωm range are, however, not always indicative of quick clay as silt and fine-grained boulder clay / glacial till may also have similar resistivity values. Also, quick clay may become non-quick with further leaching as more stabilizing ions begin to dominate the pore water (Solberg *et al.* 2008). In this case the concentration of ions may be the same as quick clay and as such the resistivity will remain in the 10–80 Ωm range. Recently, Lundström *et al.* (2009) reported that Swedish quick clays generally exhibit lower resistivity values (as low as 5 Ωm) than those from Norway and attributed this to the higher clay content generally present in Swedish clays.

The purpose of this paper is to assess the use of a number of geophysical techniques for quick clay investigations. Techniques that were used include electromagnetic conductivity mapping, Electrical Resistivity Tomography (ERT), seismic refraction and Multichannel Analysis of Surface Waves (MASW). Although the use of geoelectrical measurements has received some attention in the literature, as described above, most of these papers have focussed on ERT, with Solberg *et al.* (2008) also making use of Induced Polarization (IP) for differentiating between bedrock and sediments and seismic refraction. Electromagnetic conductivity mapping has, in contrast only received limited attention for investigating quick clay (e.g., Calvert and Hyde 2002).

Bjerrum (1954) showed that leaching may also result in a reduction of the undisturbed shear strength of marine clay. There does not, however, appear to be any information published on the effect of leaching on intact stiffness. Seismic methods were used, therefore, in order to determine the depth to bedrock and to investigate the effect (if any) of quick clay on shear-wave velocity ($V_s$). $V_s$ is related to the small strain shear stiffness ($G_{max}$, in units of Pa) by:

$$G_{max} = \rho.V_s^2 \tag{1}$$

where $\rho$ = density (kg/m$^3$).

MASW has previously been used successfully by Long and Donohue (2007, 2010) and Donohue and Long (2010) on a range of Norwegian marine clays and by Donohue *et al.* (2011) for investigating landslides.

**SETTING**

**Site description**

The Smørgrav test site is located approximately 65 km west of Oslo (Fig. 1), just east of the town of Vestfossen within the municipality of Øvre Eiker and the county of Buskerud in southeastern Norway. The site is located between 4–28 m above the present sea level and as shown, has a designated quick clay hazard level of high according to the Norwegian Water Resources and Energy Directorate (NVE) and the Geological Survey of Norway (NGU) (see http:/www.skrednett.no). The site is divided into two distinct areas, approximately 300 m apart (Fig. 2). Area 1, which has previously been investigated by NGI (Helle *et al.* 2009), is where most of the work detailed in this paper was located. This area is sloping to the NW, towards Vestfosselva (the Vestfoss river). Area 2, to the west, is the site of a quick clay landslide that occurred in 1984 (NGI 1985). The slide scar resulting from this slide is indicated in Fig. 2.

In addition to the geophysical measurements described in this paper a series of rotary pressure soundings (from Helle *et al.* 2009) and cone penetration tests (CPT's) were also performed on
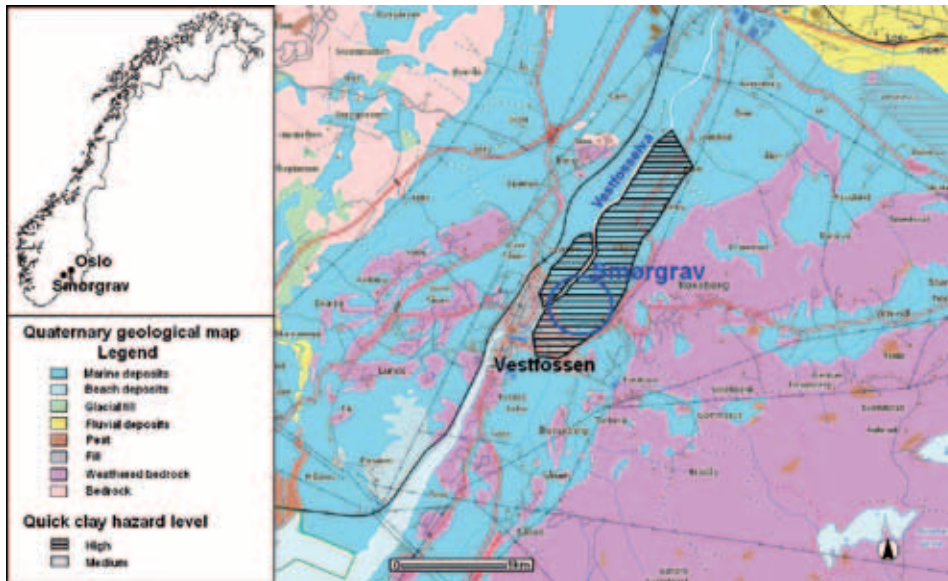
site (see Fig. 2 for locations). These data will be compared to the geophysical results.

### Geology

South-eastern Norway, in which the Smørgrav site is situated, has undergone significant isostatic uplift following deglaciation of the region about 11 000 years ago. Kenney (1964) discussed sea-level movement and the geological history of the post-glacial marine soils in the Oslo area and concluded that this region has been rising steadily with respect to sea level and that the soils were deposited during a single period of submergence. Therefore, it would be expected that the soils would be essentially normally consolidated except perhaps for some surface weathering and desiccation.

In Smørgrav, the marine limit (highest post-glacial sea level) was at about 150 m above its present level (Sørensen 1979). As shown in Fig. 1, the quaternary geology in the area around the site is dominated by marine deposits. Bedrock in the area is predominantly migmatite although to the SE there is a geological contact with phyllite (from the Geological Survey of Norway (NGU), www.ngu.no)

A soil profile is provided in Fig. 3 (from Helle *et al*. 2009), based entirely on laboratory tests for borehole 505 (see Fig. 2). As shown, between 5–13 m the material has negligible remoulded strength and this results in a zone of very high sensitivity, in excess of 30. The material between these depths also exhibits a considerably lower liquid ($W_L$) and plastic ($W_P$) limit than the overlying and underlying material. The liquid limit values are also less than the natural water content of the clay. The salt content of the quick clay increases from 1.3 g/l at 5 m depth to 4.1 g/l at 13 m depth and is generally between the 2 g/l limit suggested by Torrance (1974) and 5.6 g/l as indicated by Andersson-Sköld *et al*. (2005). It appears that this material clearly falls into the category of 'quick clay'.

## GEOPHYSICAL ACQUISITION PARAMETERS
### Electromagnetics

An electromagnetic survey, using a Geonics EM-31 electromagnetic induction meter was carried out in Area 1 (Fig. 2). The EM-31 system operates at a fixed frequency of 9.8 kHz with a fixed distance of 3.66 m between the transmitter and receiver (Geonics 1984). The survey was carried out at walking pace using the vertical magnetic dipole configuration and data from the quadrature and in-phase components of the electromagnetic field were recorded at 2 s intervals, corresponding to a sampling interval of approximately 1 m. Most of the survey was conducted in NE-SW trending transects with an inter-transect spacing of approximately 10 m. This enabled a qualitative map of the distribution of appar-
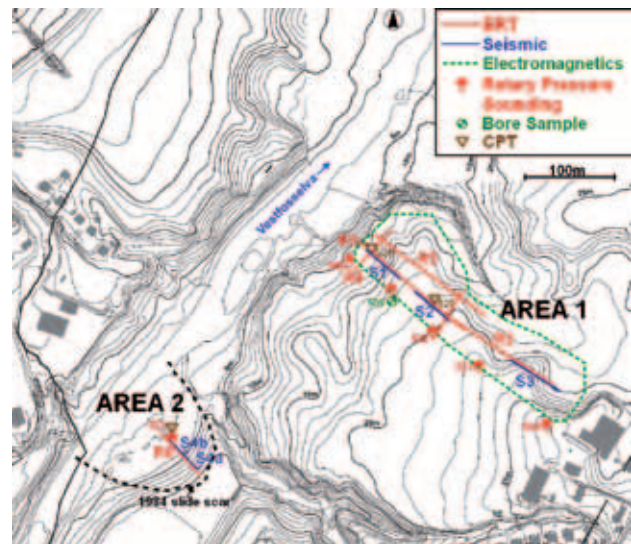


FIGURE 2
Locations of geophysical and geotechnical investigations in the study area. Contour lines: 1 m.
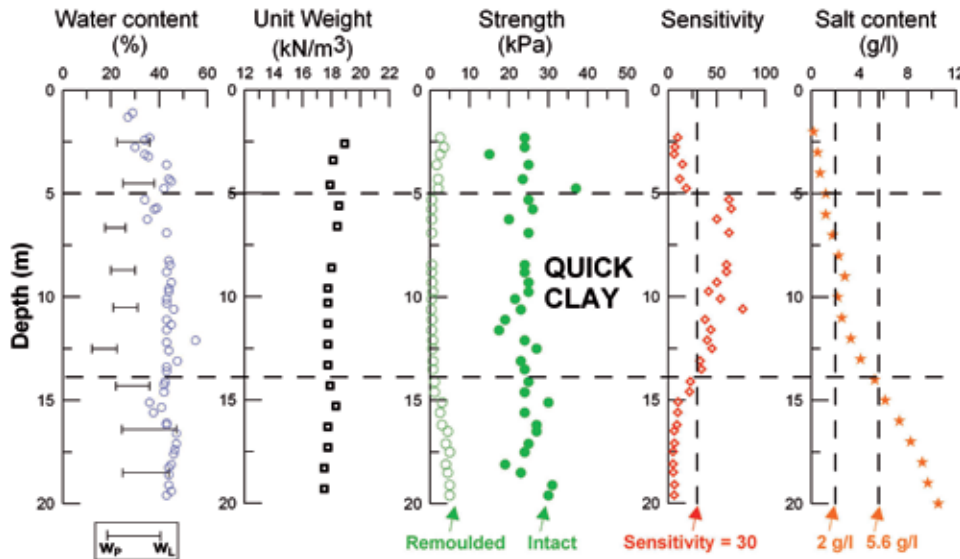
FIGURE 3

Soil profile from borehole 505 in Area 1 (Helle *et al.* 2009), see Fig. 2 for location. Where $w_p$ = plastic limit; $w_L$ = liquid limit. 2 g/l and 5.6 g/l salt content limits suggested by Torrance (1974) and Andersson-Sköld *et al.* (2005) respectively are shown. Note: water content is indicated by open blue circles and strength measurements were obtained from fall cone tests.

ent electrical conductivity (ECa) for the upper 6 m (approximately) of the subsurface to be obtained. This approach was also used as a quick reconnaissance tool in order to assist selection of appropriate locations for ERT and seismic profiles.

**Electrical Resistivity Tomography (ERT)**
Two-dimensional (2D) ERT surveys were performed along five profiles in Area 1 (R1–R5) and one profile in Area 2 (R6). Profiles R1, R2, R5 and R6 were performed uphill, approximately perpendicular to the Vestfoss river (Fig. 2), whereas R3 and R4 were approximately parallel to the river. Profiles R1 and R2 are also located close to and approximately parallel to a line of rotary pressure soundings performed by Helle *et al.* (2009). As the marine clay deposit had been shown in previous investigations to be quite thick (> 20 m in some locations), it was necessary to perform a number of deeper profiles with a 5 m electrode spacing (R1, R2 and R5), which limited the vertical and horizontal resolution. Data were acquired using a multi-electrode Campus Tigre resistivity meter with a 32 takeout multicore cable and 32 conventional stainless steel electrodes. A Wenner alpha array was used since subsurface layers were not expected to deviate significantly from the horizontal and it generally provides a good signal-to-noise ratio. This array has also been successfully used in similar

studies (Solberg *et al.* 2008). A summary of the basic resistivity acquisition parameters is provided in Table 1.

Inversion of the apparent resistivity data was carried out with the software Res2Dinv (Loke 2004) using the $L_2$ norm inversion optimization method. Due to the large subsurface resistivity contrast present at the site the quasi-Newton least squares method (Loke and Barker 1996) was not deemed appropriate, instead the Gauss-Newton method (Sasaki 1989; deGroot-Hedlin and Constable 1990) was selected for the first 2 or 3 iterations, after which the quasi-Newton method was used. In many cases, this provides the best compromise between computational time and accuracy even at sites with large resistivity contrasts (Loke and Dahlin 2002). For this study, all inversions performed converged to a normalized root-mean-squared (RMS) error of less than 5% within 5 iterations.

The 2D ERT profiles from Area 1 were then combined using the software Rockworks into a quasi 3D fence diagram, in order to provide an indication of the 3D distribution of resistivity.

**Seismic refraction and Multichannel Analysis of Surface Waves (MASW)**
Seismic refraction and MASW profiles were both performed along lines, S1, S2, S4 and S5 (Fig. 2), all approximately perpen-

TABLE 1

ERT data acquisition parameters

| Profile | Array Type | Profile Length (m) | Electrode Spacing (m) |
|---------|-----------|--------------------|-----------------------|
| R 1 | Wenner α | 155 | 5 |
| R 2 | Wenner α | 155 | 5 |
| R 3 | Wenner α | 62 | 2 |
| R 4 | Wenner α | 62 | 2 |
| R 5 | Wenner α | 155 | 5 |
| R 6 | Wenner α | 62 | 2 |

TABLE 2
Seismic data acquisition parameters. Note: (o) refers to seismic refraction offshoots.

| Profile | Type | Num. Geophones | Geophone Spacing (m) | Record Length (s) | Source Locations |
|---------|------|----------------|----------------------|-------------------|------------------|
| S 1 | Refraction | 24 | 2 | 0.1 | G (Geophone)1+27m (o), G1, G6, G12, G18, G24, G24+30m (o) |
|  | MASW | 24 | 2 | 1 | G1, G1+4m, G1+8m, G24, G24+4m, G24+8m |
| S 2 | Refraction | 24 | 2 | 0.1 | G1 + 30m (o), G1, G6, G12, G18, G24, G24+30m (o) |
|  | MASW | 24 | 2 | 1 | G1, G1+4m, G1+8m, G24, G24+4m, G24+8m |
| S 3 | Refraction | 24 | 3 | 0.1 | G1+27m (o), G1, G6, G12, G19, G24, G24+30m (o) |
| S 4 | Refraction | 24 | 2 | 0.1 | G1+20m (o), G1, G6, G12, G18, G24, G24+7m |
| S4a | MASW | 12 | 2 | 1 | G1, G1+4m |
| S4b | MASW | 12 | 2 | 1 | G1, G1+4m |

dicular to the river. Only seismic refraction was performed in-line S3. The seismic data were recorded using a Geometrics Geode seismograph (with 24 geophones). A 10 kg sledgehammer was used to generate the seismic waves, which were in turn detected by 10 Hz vertical geophones. A geophone spacing of 2 m was used for all profiles except S3, where a 3 m spacing was used. In general, for seismic refraction testing, shots (hammer blows) were recorded at every sixth geophone, with offshots recorded off each end of the profile. Acquisition parameters are reported in Table 2. An example of a shot gather acquired on site is shown in Fig. 4(a), together with the picked first-arrival times. Clear and unambiguous first arrivals were observed on all of the acquired profiles. Example traveltime–distance (T–X) curves are given in Fig. 4(b). The refraction data were interpreted using GREMIX, which incorporates the slope-intercept method, parts of the Plus-Minus Method of Hagedoorn (1959), Time-Delay Method (see Wyrobek 1956) and features the Generalized Reciprocal Method (GRM) of Palmer (1980).

As recommended by Donohue and Long (2008), a number of different source locations were chosen for each MASW profile to determine the optimum acquisition parameters (i.e., to minimize near-field effects), at a number of source-receiver offsets (Table 2). Processing of the MASW data was performed by selecting dispersion curves from a phase velocity-frequency spectra, generated using a wavefield transformation method (McMechan and Yedlin 1981; Park *et al*. 1999). 1D shear-wave velocity models were estimated using the least squares approach of Xia *et al*. (1999). A number of different initial models with different numbers of layers were selected in the initial model in order to test the robustness of the inversion and to determine the model with the lowest misfit. In order to reduce the non-uniqueness of the inversion, P-wave velocities from the seismic refraction surveys were included as *a priori* information. Following the recommendations of Cercato (2009) and Luke and Calderón-Macías (2007) the layer thickness in the model was increased exponentially with depth. This reflects the fact that the resolving power of MASW data decreases with depth. Each inversion was allowed a sufficient number of iterations to converge and was

stopped after the overall RMS error was less than 2 m/s. All of the inversions performed converged rapidly, usually within 3 iterations. It was consistently found that a ten layer initial model produced the lowest RMS error. Additional layers produced similar errors, however these resulted in over-parametrized inversions, as evidenced by inversion artefacts such as 'smoothing' over the layer boundaries as well as artefact low velocity layers, not supported by evidence from the local geology.

## RESULTS AND DISCUSSION
### Area 1
*In-situ geotechnical testing*
The rotary pressure sounding results and interpretations, shown in Fig. 5 (from Helle *et al*. 2009) indicate a layer of quick clay where the penetration resistance curves are vertical or almost
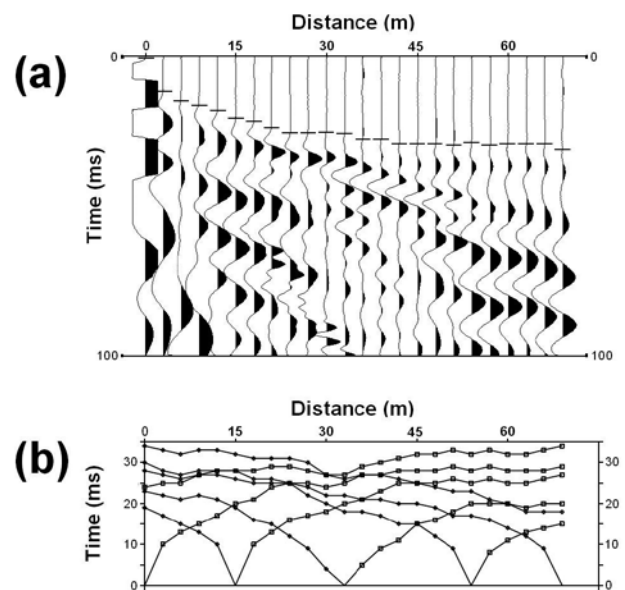


FIGURE 4
Sample seismic refraction shot gather for profile S3 with picked first arrival times (a) and example traveltime-distance curves, also for S3 (b).
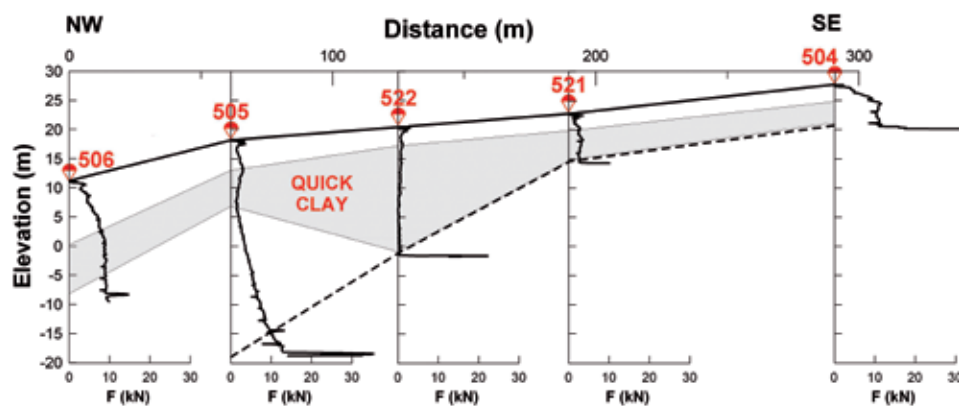
vertical (Rygg 1988). The thickness of this layer appears to vary considerably over the length of the section with the thickest area of quick clay located at rotary pressure sounding 522.

The results of two Cone Penetration Tests (CPT's), from this area are provided in Fig. 6. These CPT's are located very close to seismic profile lines S1 and S2 (Fig. 2) and were chosen following interpretation of the rotary pressure sounding, electromagnetics and ERT results. CPT 524 was performed in the zone interpreted to contain non-quick clay whereas CPT 525 was performed where quick clay was thought to be present. As shown, in terms of corrected cone resistance ($q_t$) both profiles are similar, except between 1.5–9 m depth where CPT 525 (in quick clay) produces slightly lower values (approximately 0.2 MPa lower). In terms of sleeve friction ($f_s$) a small difference (up to a maximum of 7 kPa) is observed between the two CPT's at depths in excess of 4 m. Following the discussion of Rankka *et al.* (2004), it was not expected that the sleeve friction ($f_s$) would be able to distinguish between quick and non-quick clay. Due to its location close to the cone, it was expected that the clay would not be fully remoulded at the sleeve. In general, this will limit the use of this measurement for providing an indication of sensitivity (Rankka *et al.* 2004).

### Electromagnetics

The results for the electromagnetic survey are shown in Fig. 7 for the quadrature component of the electromagnetic field. It should be noted that EM-31 provides a measurement of conductivity within 6 m of the surface and therefore can only give an indication of the clay 'outcropping' just below the dry-crust. As a result quick-clay layers below this depth may remain undetected. An EM-34 instrument (or equivalent) with a longer coil separation would be more suitable for investigating deeper deposits, however, this would result in a reduction in resolution. As shown, there is a contrast in the apparent conductivity measured in the NW compared to the measurement elsewhere in the survey, with significantly higher conductivities (up to 80 mS/m) measured in this area. This could possibly be interpreted as an increase in salinity, thereby indicating the presence of an unleached or non-quick material. Electrical services (the location of which were

known in advance of testing), were also detected using this approach and are observed in Fig. 7 as a NE-SW trending anomaly.

### Electrical Resistivity Tomography (ERT) compared to bore data

A combined inversion of the collinear and overlapping profiles R1 and R2 was performed, the results of which are shown in Fig. 8. As illustrated, there is a reasonably consistent upper layer of relatively high resistivity, approximately 2 m thick, which corresponds to the dry upper crust. Below this thin crustal layer there appears to be a contrast in resistivity (similar to that observed in the EM data, above), with higher values (>100 Ωm) measured in the SE (uphill) and becoming very low (1–10 Ωm) in the NW (river end). According to the criterion of Solberg *et al.* (2008), inverted resistivity values in the 10–80 Ωm range may indicate quick clay.

Although Occam-style inversion models are generally ill-suited for detecting discrete geological boundaries (Nguyen *et al.* 2005), in this case, however, comparison with the rotary pressure sounding results (Fig. 5) and the geotechnical laboratory testing
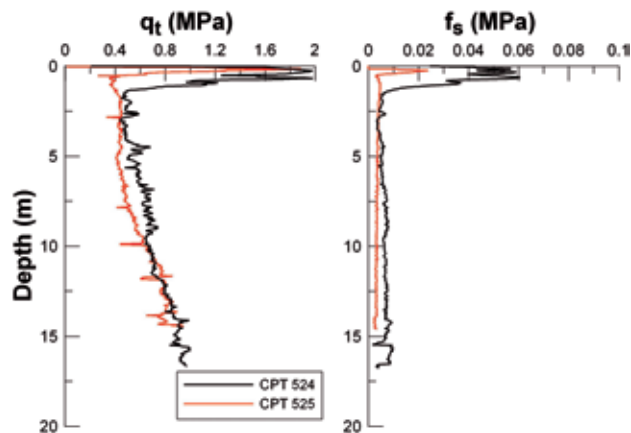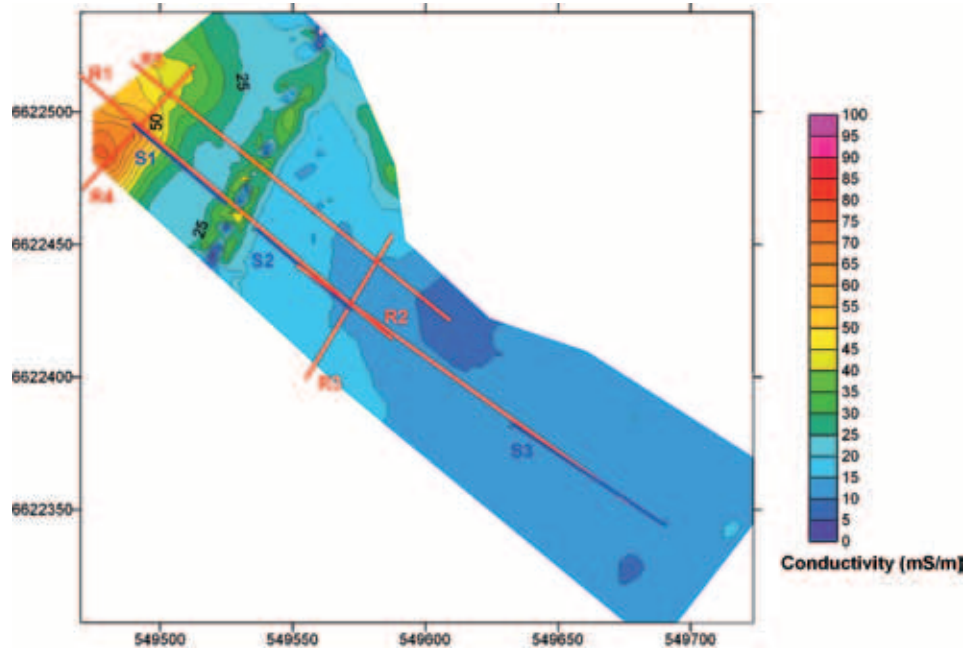


FIGURE 6
Corrected cone resistance ($q_t$) and sleeve friction ($f_s$) results for CPT 524 and CPT 525 (see Fig. 2 for location).

FIGURE 7

EM-31 survey results along with the corresponding locations of ERT and seismic profile lines. See Fig. 2 for location of the EM-31 survey.



of samples (Fig. 3) indicate the highlighted resistivity contours in Fig. 8 as a likely interface between unleached and quick clay. In addition, Helle *et al*. (2009) measured resistivity both on borehole samples (from borehole 505, Fig. 2) and using a CPT with a four electrode array incorporated into a rod behind the cone. They measured similar resistivity values with both approaches to those measured following inversion of the ERT data in this study. These results suggest that quick clay investigations using discrete rotary pressure soundings can be significantly enhanced by using ERT profiles to interpolate between soundings. For example, from the rotary pressure sounding results (Fig. 5), quick clay could be interpreted as being present between soundings 505 and 506. The ERT data, however, suggest that this area predominantly contains non-quick clay, with a resistivity of less than 10 Ωm. This high-lights the potential benefits of using ERT profiles to interpolate between test locations, perhaps significantly reducing the need for large numbers of soundings.

The geotechnical parameters measured on samples from borehole 505 (Fig. 3) are generally in agreement with the resis-tivity measurements at that location. As discussed above, quick clay was confirmed between 5–13 m depth in this borehole. The corresponding inverted resistivity at this depth varies between 10–30 Ωm, which is within the range suggested by Solberg *et al*. (2008). Below this depth the salt content (Fig. 3) increases con-siderably (as the clay is unleached) and the corresponding resis-tivity values drop to less than 7 Ωm.

As the focus of this paper is on quick clay, the resistivity scale shown in Fig. 8 has a limited range, it should be noted, however, that the resistivity values detected in the SE are in excess of 1000 Ωm suggesting shallow bedrock in this area. This is also indicated by the significant increase in pushing force recorded for rotary pressure soundings 521 and 504 at shallow depth (Fig. 5). The thickest area of quick clay according to both the ERT and rotary pressure sounding approaches appears to be located close to this suggested bedrock surface. Early work by Løken (1968) showed that the leaching rate is at its highest close
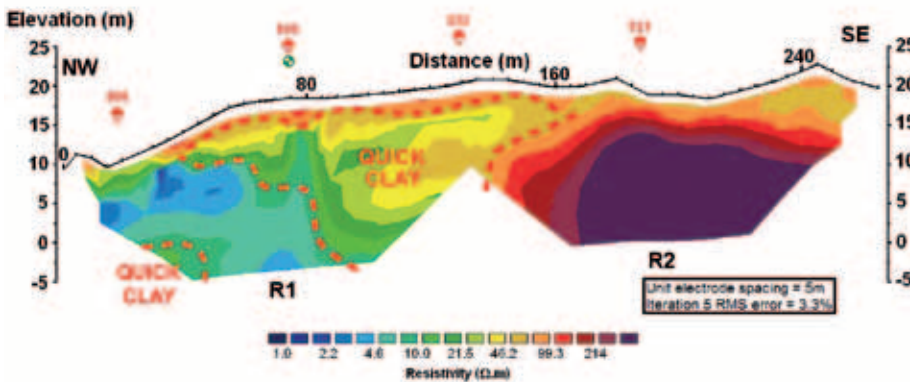


FIGURE 8

Electrical resistivity tomography results for the combined inversion of profiles R1 and R2, along with interpreted extent of quick clay.
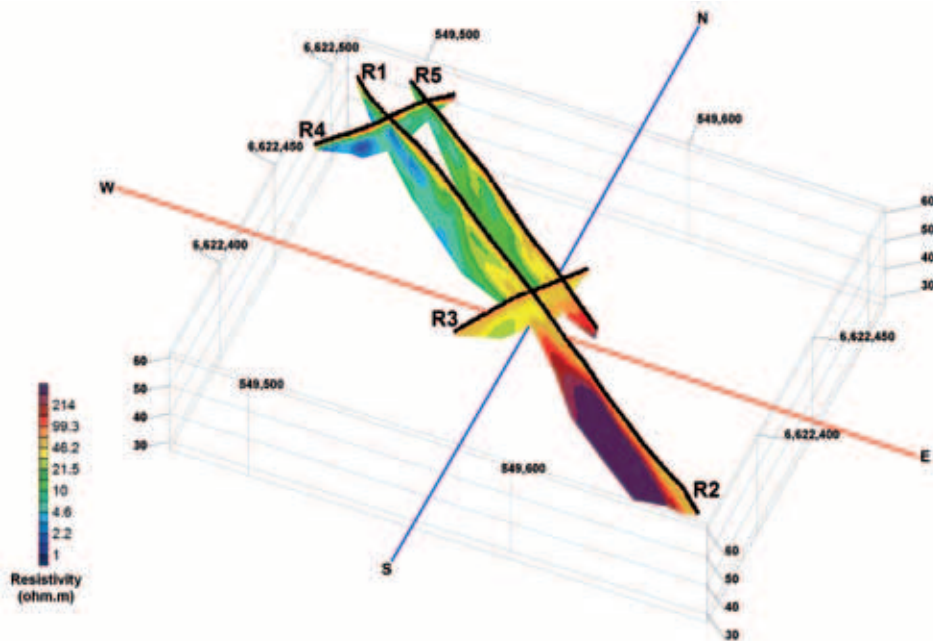
FIGURE 9

Fence diagram, combining all ERT profiles for Area 1.

to bedrock. Bedrock will influence the nature of local drainage and therefore its location will have a significant effect on the formation of quick clay.

A 3D fence diagram, combining the 2D ERT profiles from Area 1, is shown in Fig. 9. Note the contrast in resistivity between parallel profiles R3 and R4. For R4, beneath the high resistivity crustal layer, the resistivity values are in general very low (1–10 Ωm). This supports the findings of the EM-31 survey and indicates the presence of unleached marine clay. As shown, the interpreted layer of quick clay in the centre of this fence diagram (10–80 Ωm) is consistent across the intersecting ERT profiles.

**Seismic refraction and MASW**

The interpreted seismic refraction layered models for profiles S1, S2 and S3 are overlain on ERT profiles R1 and R2 in Fig. 10. As shown, S1 is predominantly located at the region of low resistivity, possibly unleached material, whereas S2 is located at the zone where resistivity values were measured in the expected

quick clay range (see Fig. 8). Two thin crustal layers were detected on each of these profiles with velocities less than 1000 m/s. Below this, a P-wave velocity (Vp) layer of 1500 m/s was detected on profiles S1 and S2, which corresponds to the marine clay observed in the borehole and resistivity data. A $V_p$ of 4600 m/s was detected as the deepest layer on S3, which supports the interpretation of shallow bedrock in this area, also indicated by the rotary pressure soundings and ERT profiles. As discussed above, knowledge of the location of bedrock is important in quick clay investigations due to its influence on local drainage (Løken 1968).

Surface wave shot gathers, corresponding dispersion images and dispersion curves are illustrated in Fig. 11 for profiles S1 and S2. A normally dispersive phase velocity-frequency relationship is observed for both S1 and S2 (Fig. 11b and Fig. 11e), dominated by the fundamental mode Raleigh wave. There appears to be some difference in the raw shot gathers, which manifests itself as greater dispersion at low frequencies (<5 Hz)
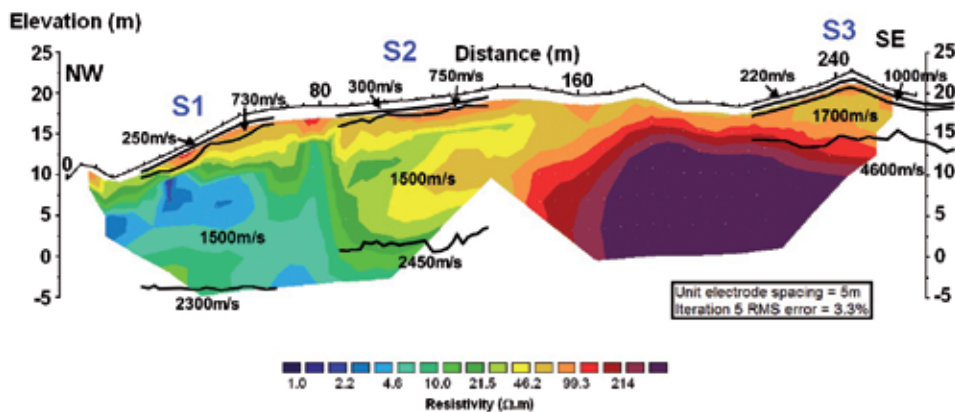


FIGURE 10

Interpreted P-wave velocity refraction models overlain on resistivity profiles R1 and R2.

in the dispersion image for S1. Shear-wave velocity ($V_s$) profiles for S1 and S2, produced following inversion of the preferred dispersion curves at peak amplitude (Fig. 11b and Fig. 11e) are illustrated in Fig. 12. Interestingly, profile line S2, which is located over quick clay, exhibits lower inverted velocities between 1.2–9.7 m. This compares well to the reduced CPT $q_t$ values observed between 1.5–9 m depth (Fig. 6). The greatest difference between the two MASW profiles was observed between 1.8–5.5 m depth. Here the difference between profiles is as great as 17 m/s, which corresponds to a difference in $G_{max}$ (equation (1)) of about 8 MPa. This difference is close to the expected uncertainty reported by Asten and Boore (2005), Xia *et al*. (2002) and Moss *et al*. (2008) when comparing MASW $V_s$ measurements with those from a range of other techniques. As the same inversion parameters were used for both profiles the most likely source of relative uncertainty in the inverted $V_s$ profiles is related to picking of the dispersion curves. Although the peak amplitude/spectral maxima is assumed to be the correct dispersion curve location, some ambiguity exists at low frequencies (Fig. 11). As described by Lai *et al*. (2005), the dispersion curves appear to be separated in two regions, at higher frequencies where the uncertainty is lower, and at lower frequencies (< 11 Hz) where uncertainty is greater. In order to quantify this uncertainty two further dispersion curves were picked from both dispersion images shown in Fig. 11, relating to the minimum and maximum phase velocities that could be picked on opposite sides of the coherent peak. Following inversion of these curves it is observed that uncertainty increases considerably at depths in excess of 7.5 m (Fig. 12), up to a maximum coefficient of variation (standard deviation normalized by the mean) of 6%. Above 5.5 m, where most of the difference between profiles is observed, there appears to be minimal uncertainty in $V_s$ related to picking of the dispersion curve (coefficient of variation <2 %).

## Area 2

### In-situ geotechnical testing

CPT and rotary pressure sounding 523, situated in the slide scar (Fig. 2), indicates non-sensitive clay/slide material (Fig. 13) down to an elevation of 0 m (3.6 m depth). The corrected cone resistance measured in the slide deposits (Fig. 13a) is significantly higher than that measured for the intact clay in Area 1 (Fig. 6). According to Janbu (1974), Mitchell (1993) and Ter-Stepanian (2000), this is likely due to an increase in the remoulded strength following con-
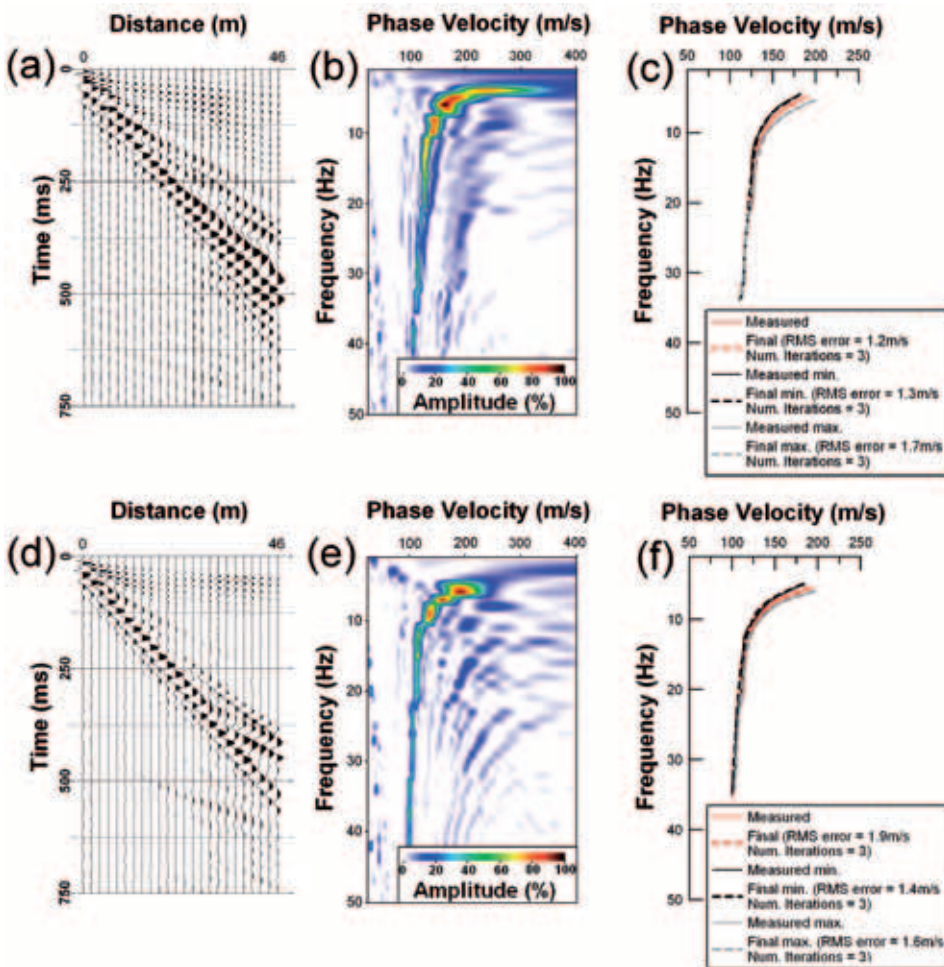


FIGURE 11

Shot gather, dispersion image and dispersion curves with associated Root Mean Square (RMS) error for S1 (a,b,c) and S2 (d,e,f). Minimum and maximum dispersion curves are shown corresponding to phase velocities picked on opposite sides of the coherent peak.
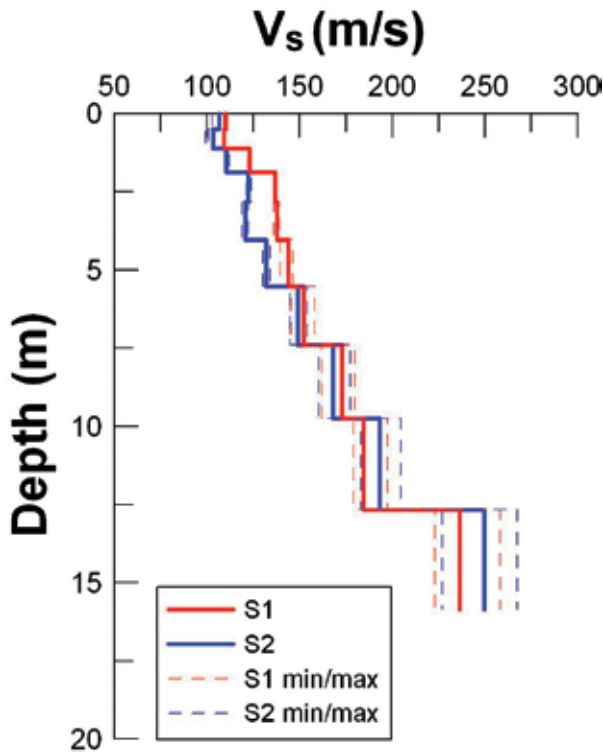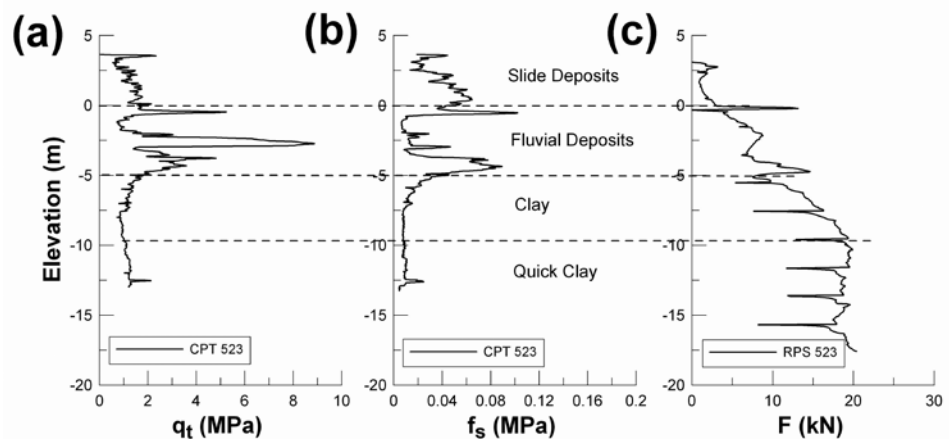
FIGURE 12 Shear-wave velocity profiles for S1 and S2 produced following inversion of the preferred dispersion curves at peak amplitude (Fig. 10b and Fig.10e) along with profiles produced following inversion of minimum and maximum dispersion curves.

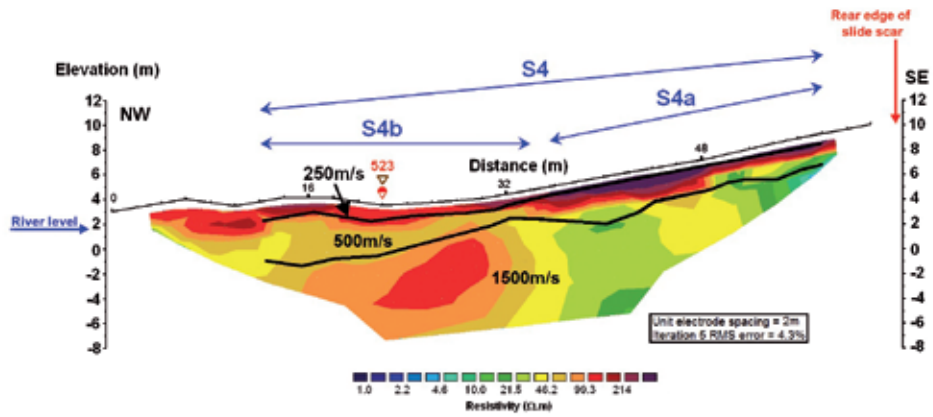**Electrical Resistivity Tomography (ERT) compared to bore data**

The inverted resistivity profile R6, in the scar of the 1984 quick clay slide, is shown in Fig. 14. The profile shows a ca. 2 m thick laterally consistent top layer of high resistivity, which according to NGI (1985), was fill placed there following the landslide. Below, the SE part has low resistivity values, while the NW part shows relatively high values (40–70 Ωm). When compared to the CPT and rotary pressure sounding data, this material is interpreted to be remoulded slide deposits. These values are lower than those reported by Solberg *et al*. (2008) for slide deposits and are in a similar range (although on the high end) to those expected for quick clay. Below this layer, the fluvial deposits interpreted from the CPT data exhibit higher resistivities (70–200 Ωm). Unfortunately, due to site constraints the ERT profile could not be extended sufficiently to detect the quick clay observed by the rotary pressure sounding at depth. The SE part of the resistivity profile indicates quick clay (10–50 Ωm).

**Seismic refraction and MASW**

The interpreted seismic refraction layered models for profile S4 is overlain on ERT profile R6 in Fig. 14. Two shallow layers with velocities of 250 m/s and 500 m/s were detected and these overlay a layer of 1500 m/s. When compared to the CPT and rotary pressure sounding results it appears that the boundary between 500–1500 m/s possibly reflects the base of the slide deposits and the failure surface of the slide. No distinction in P-wave velocity was observed between the fluvial deposits in the NW and the lower resistivity (assumed quick clay material) in the slope.

For the purposes of MASW testing, profile S4 was subdivided into two separate 12 geophone lines, which were acquired and processed separately, in order to provide shear-wave velocity profiles for both the material in the slope (S4a) and the remoulded slide mass (S4b) (see Fig. 14). As shown in Fig. 15, the dispersive images and corresponding picked dispersion curves are significantly different for these two profiles. The resultant inverted $V_s$ values (Fig. 16) for the remoulded material are significantly higher than those measured for the material in the

solidation of the remoulded quick clay deposit since the failure occurred in 1984. The material directly underlying these slide deposits exhibits higher cone resistances. According to the Robertson (1990) CPT material classification chart this material should be classified as sand or silty sand. Due to its proximity to the Vestfoss river it is likely therefore that this material is fluvial in origin. This material appears to overlay low sensitivity clay, which in turn overlies quick clay as the rotary pressure sounding penetration resistance curve is close to vertical (Fig. 13c).



FIGURE 13 Corrected cone resistance (a) and sleeve friction (b) results for CPT 523 along with rotary pressure sounding 523 (from Helle *et al*. 2009) (c). See Fig. 2 for locations.

FIGURE 14
Resistivity profile R6 with inter-
preted P-wave velocity refraction
model.



slope. As discussed above, CPT resistances were also relatively high for the slide deposits, possibly due to an increase in the remoulded strength following consolidation since the failure occurred (Janbu 1974; Mitchell 1993; Ter-Stepanian 2000).

**CONCLUSIONS**

The main objective of this work was to assess a number of geophysical techniques for use in quick clay investigations. A number of these approaches have proved promising and it was found that:

• the EM-31 electromagnetic survey detected an area of very high conductivity in the NW of Area 1, corresponding to unleached marine clay. It should be noted that EM-31 only provides a bulk measurement of conductivity within 6 m of the surface and therefore can only give an indication of the clay 'outcropping' just below the dry-crust. Its use will therefore be limited where deeper layers of quick clay are present. On this occasion, however, it was found to be a useful reconnaissance tool and assisted the design of the rest of the geophysical and geotechnical surveys.
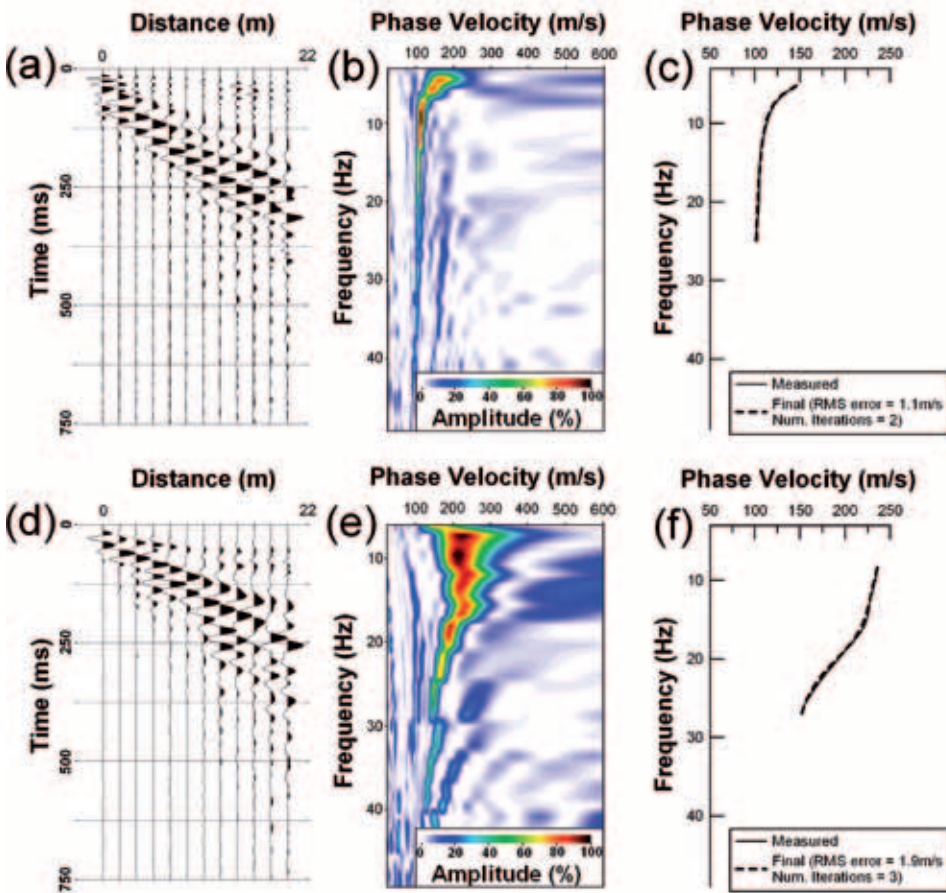


FIGURE 15 Shot gather, disper-
sion image and dispersion curve
with associated RMS error for
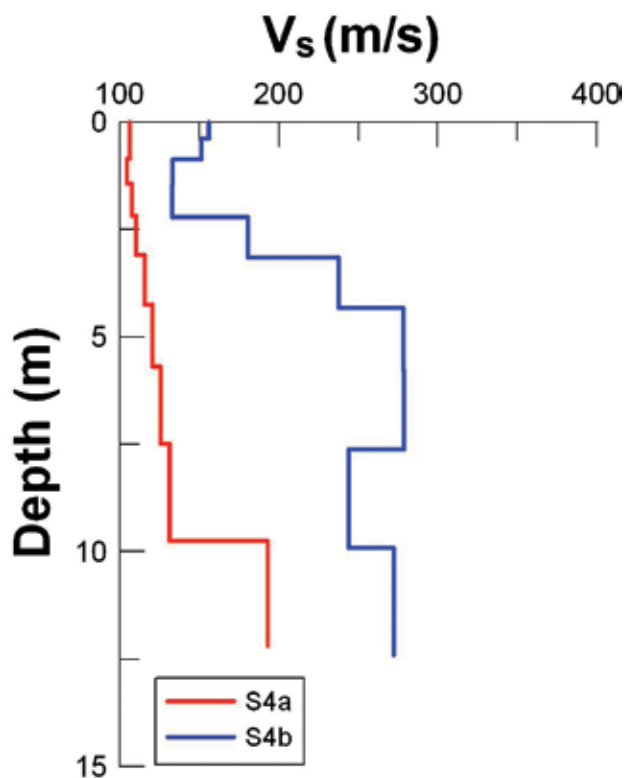S4a (a,b,c) and S4b (d,e,f).

**FIGURE 16**
Inverted shear-wave velocity profiles for S4a and S4b.

- as expected, the Electrical Resistivity Tomography (ERT) approach proved to be the most successful of all the geophysical techniques tested. An extensive amount of clay with a resistivity of 10–80 Ωm was observed on site, indicating quick clay. This interpretation was strengthened by bore samples and rotary pressure soundings. It should be noted, however, that resistivity values in this range are only indicative of quick clay, as silt, fine-grained boulder clay/glacial till and as discovered here, quick clay slide deposits, may also produce similar resistivity values. It is recommended, therefore, that ERT or other resistivity measurements should not be used as a replacement for rotary pressure soundings or other geotechnical testing. The results from this work are in agreement with those of Solberg *et al.* (2008) who suggested that quick clay investigations using discrete rotary pressure soundings can be significantly enhanced by using 2D or more detailed 3D ERT profiles to interpolate between soundings, perhaps significantly reducing the need for large numbers of soundings. The use of modern continuous resistivity systems could prove useful for high speed data acquisition, although galvanically coupled systems such as PACES (e.g., Sørensen 1996) would likely perform better than capacitively coupled systems in light of the highly conductive marine clay. Also the use of induced polarization should be further explored for distinguishing quick clay.

- P-wave seismic refraction was useful for determining the soil distribution as well as for indicating the presence of shallow bedrock to the SE in Area 1. Shear-wave velocities for quick clay, measured using the MASW approach in Area 1, appear to be slightly less (up to 17 m/s) than those measured for unleached clay to a depth of 9 m. Minimal uncertainty in $V_s$, related to picking of the dispersion curve, is observed above 5.5 m, however, it starts to become increasingly significant below this depth where the difference between $V_s$ profiles cannot be relied upon. Further work is necessary in order to fully investigate the effect of leaching on $V_s$ (and corresponding small strain stiffness). $V_s$ values for the remoulded slide deposits in Area 2 were found to be significantly higher than those measured on intact quick or unleached deposits. This is due to an increase in density and strength of the material following remoulding and subsequent consolidation. As with ERT, described above, high speed roll-along acquisition of MASW data using a streamer (e.g., Luo *et al.* 2008; Long *et al.* 2009), for production of 2D $V_s$ profiles could prove useful for improving site characterization in areas of quick clay.

## REFERENCES

Andersson-Sköld Y., Torrance J.K., Lind B., Odén K., Stevens R.L. and Rankka K. 2005. Quick clay – A case study of chemical perspective in Southwest Sweden. *Engineering Geology* **82**, 107–118.

Asten M.W. and Boore D.M. 2005. Comparison of shear-velocity profiles of unconsolidated sediments near the Coyote borehole (CCOC) measured with fourteen invasive and non-invasive methods, U.S. Geological Survey Open-File Report. 2005–1169.

Bjerrum L. 1954. Geotechnical properties of Norwegian marine clays. *Géotechnique* **4**, 49–69.

Brenner R.P., Nutalaya P., Chilingarin G.V. and Robertson J.D. 1981. Engineering geology of soft clay In: *Soft Clay Engineering* (eds. E.W. Brand and R.P. Brenner), Elsevier, Amsterdam, 159–240.

Calvert H.T. and Hyde C.S.B. 2002. Assessing landslide hazard in the Ottawa Valley using electrical and electromagnetic methods. *Proceedings of the Symposium on the Application of Geophysics to Engineering and Environmental Problems (SAGEEP),* February 10–14, 2002, Las Vegas, Nevada. Environmental and Engineering Geophysical Society, Wheat Ridge, Colorado.

Cercato M. 2009. Addressing non-uniqueness in linearized multichannel surface wave inversion. *Geophysical Prospecting* **57**, 27–47.

Dahlin T., Larsson R., Leroux V., Larsson R. and Rankka K. 2005. Resistivity imaging for mapping of quick clays for landslide risk assessment. *Proceedings of 11th Annual Meeting EAGE – Environmental and Engineering Geophysics*, Palermo, Italy, 4–7 September 2005. A046.

Donohue S. and Long M. 2008. An assessment of the MASW technique incorporating discrete particle modelling. *Journal of Environmental and Engineering Geophysics* **13**(2), 57–68.

Donohue S. and Long M. 2010. Assessment of sample quality in soft clay using shear wave velocity and suction measurements. *Géotechnique* **60**(11), 883–889. doi: 10.1680/geot.8.T.007.3741

Donohue S., Tolooiyan A. and Gavin K. 2011. Geophysical and geotechnical assessment of a railway embankment failure. *Near Surface Geophysics* **9**(1), 33–44. doi: 10.3997/1873-0604.2010040

Geonics Ltd. 1984. Operating manual for EM-31-D non-contacting terrain conductivity meter. Geonics, Ltd., Toronto, Ontario, Canada.

Göransson G.I., Bendz D. and Larson P.M. 2009. Combining landslide and contaminant risk: A preliminary assessment. *Journal of Soils and Sediments* 933–45. doi: 10.1007/s11368-008-0035-z

Gregersen O. 1981. The quick clay landslide in Rissa, Norway. Contribution to the 10th International Conference on Soil Mechanics and Foundation Engineering, Stockholm. Norwegian Geotechnical Institute 135, 6p.

deGroot-Hedlin C. and Constable S. 1990. Occam's inversion to generate smooth, two-dimensional models form magnetotelluric data. *Geophysics* **55**, 1613–1624.

Hagedoorn J.G. 1959. The plus-minus method of interpreting seismic refraction sections. *Geophysical Prospecting* **7**, 158–182.

Helle T.E., Pfaffhuber A.A., Rømoen M. and Forsberg C.F. 2009. SIP12 – Correlation between horizontal and vertical resistivity measurements. NGI Report 20081135-1.

Helle T.E., Pfaffhuber A.A., Rømoen M., Løken T. and Karlsrud K. Resistivity logging (RCPTU) to delineate quick clay, assessed by geochemical analysis: A Norwegian case study. Submitted to the Canadian Geotechnical Journal.

Janbu N. 1974. Written discussion to European Symposium on Penetration Testing, ESOPT-I, Stockholm, Proceedings 2.1, 132–134.

Kenney T.C. 1964. Sea-level movements and the geological histories of the post-glacial marine soils at Boston, Nicolet, Ottawa and Oslo. *Géotechnique* **14**(3), 203–230.

Lai C.G., Foti S. and Rix G.J. 2005. Propagation of data uncertainty in surface wave inversion. *Journal of Engineering and Environmental Geophysics* **10**, 219–228.

Loke M.H. 2004. Res2DInv ver. 3.54. Geoelectrical Imaging 2D and 3D. Instruction Manual. Geotomo Software.

Loke M.H. and Barker R.D. 1996. Rapid least-squares inversion of apparent resistivity pseudosections by a quasi-Newton method. *Geophysical Prospecting* **44**, 131–152.

Loke M.H. and Dahlin T. 2002. A comparison of the Gauss-Newton and quasi-Newton methods in resistivity imaging inversion. *Journal of Applied Geophysics* **49**, 149–162.

Løken T. 1968. Kvikkleiredannelse og kjemisk forvitring i norske leirer. Norwegian Geotechnical Institute, Oslo. Publication **75**, 19–26. (In Norwegian)

Long M. and Donohue S. 2007. In situ shear wave velocity from multichannel analysis of surface waves (MASW) tests at eight Norwegian research sites. *Canadian Geotechnical Journal* **44(5), 533–544.**

Long M. and Donohue S. 2010. Characterisation of Norwegian marine clays with combined shear wave velocity and CPTU data. *Canadian Geotechnical Journal* **47**(5), 709–718.

Long M., Donohue S., O'Connor P. and Quigley P. 2009. Relationship between shear wave velocity and undrained shear strength of Irish glacial tills. *Proceedings of the EAGE Near Surface 2009, 15th Annual Meeting of Environmental and Engineering Geophysics*, September. Paper A13.

Luke B. and Calderón-Macías C. 2007. Inversion of seismic surface wave data to resolve complex profiles. *Journal of Geotechnical and Geoenvironmental Engineering* **133**(2), 155–165.

Lundström K., Larsson R. and Dahlin T. 2009. Mapping of quick clay formations using geotechnical and geophysical methods. *Landslides* **6**, 1–15

Luo Y., Xia J., Liu J., Xu Y. and Liu Q. 2008. Generation of a pseudo-2D shear-wave velocity section by inversion of a series of 1D dispersion curves. *Journal of Applied Geophysics* **64**(3–4), 115–124.

McMechan G.A. and Yedlin M.J. 1981. Analysis of dispersive waves by wave field transformation. *Geophysics* **46**, 869–874.

Mitchell J.K. 1993. *Fundamentals of Soil Behavior*. John Wiley, New York

Moss R.E.S. 2008. Quantifying measurement uncertainty of thirty-meter shear-wave velocity. *Bulletin of the Seismological Society of America* **98**, 1399–1411.

NGI. 1985. Øvre Eiker kommune. Stabilitetsforholdene på Strandajordet, Vestfossen etter utglidningen den 11.september 1984 NGI-report 85002-01, dated 26.4.1985

Nguyen F., Garambois S., Jongmans D., Loke M.H. and Pirard E. 2005, Image processing of 2D resistivity data for imaging faults. *Journal of Applied Geophysics* **57**, 260–277.

Palmer D. 1980. The generalized reciprocal method of seismic refraction interpretation. Society of Exploration Geophysicists, Tulsa, OK, 104 p.

Park C.B., Miller D.M. and Xia J. 1999. Multichannel Analysis of surface waves. *Geophysics* **64** (3), 800–808.

Rankka K., Anderssen-Skold Y., Hulten C., Larsson R., Leroux V. and Dahlin T. 2004. Quick clay in Sweden. Report 65, Swedish Geotechnical Institute. Linkoping.

Robertson P.K. 1990. Soil classification using the cone penetration test. *Canadian Geotechnical Journal* **27**(1), 151–158.

Rygg N. 1988. Rotary pressure sounding: 20 years of experience. Proc. Pen Testing, 1988, ISOPT-1, DeRuiter ed., Balkema, 453–457.

Sasaki Y. 1989. Two-dimensional joint inversion of magnetotelluric and dipole-dipole resistivity data. *Geophysics* **54**, 254–262.

Söderblom R. 1969. Salt in Swedish clays and its importance for quick clay formation. Results from some field and laboratory studies. Swedish Geotechnical Institute, Proceedings 22, Stockholm.

Solberg I.L., Rønning J.S., Dalsegg E., Hansen L., Rokoengen K. and Sandven R. 2008. Resistivity measurements as a tool for outlining quick-clay extent and valley-fill stratigraphy: A feasibility study from Buvika, Central Norway. *Canadian Geotechnical Journal* **45**, 210–225.

Sørensen R. 1979. Late Weichselian deglaciation in the Oslofjord area, South Norway. *Boreas* **8**, 241–246.

Sørensen K.I. 1996. Pulled array continuous electrical profiling. *First Break* **14**, 85–90.

Ter-Stepanian G. 2000. Quick clay landslides: Their enigmatic features and mechanism. *The Bulletin of Engineering Geology and the Environment* **59**(1), 47–57.

Torrance J.K. 1974. A laboratory investigation of the effect of leaching on the compressibility and shear strength of Norwegian marine clays. *Géotechnique* **24**(2), 155–173.

Wyrobek S.M. 1956. Application of delay and intercept times in the interpretation of multi-layer refraction time distance curves. *Geophysical Prospecting* **4**(2), 112–130.

Xia J., Miller R.D. and Park C.B. 1999. Estimation of near surface shear wave velocity by inversion of Raleigh waves. *Geophysics* **64**(3), 691–700.

Xia J., Miller R.D., Park C.B., Hunter J.A., Harris J.B. and Ivanov J. 2002. Comparing shear-wave velocity profiles inverted from multichannel surface wave with borehole measurements. *Soil Dynamics and Earthquake Engineeri*ng **22**, 181–190.